arXiv:1304.3336v2 [cond-mat.mes-hall] 12 Apr 2013

Pressure induced topological quantum phase transition in Sb_2Se_3

Wei Li,[1, 2] Xin-Yuan Wei,[1] Jian-Xin Zhu,[3] C. S. Ting,[4] and Yan Chen[1]
[1]*Department of Physics, State Key Laboratory of Surface Physics and*
Laboratory of Advanced Materials, Fudan University, Shanghai 200433, China
[2]*State Key Laboratory of Functional Materials for Informatics,*
Shanghai Institute of Microsystem and Information Technology,
Chinese Academy of Sciences, Shanghai 200050, China
[3]*Theoretical Division and Center for Integrated Nanotechnologies,*
Los Alamos National Laboratory, Los Alamos, New Mexico 87545, USA
[4]*Texas Center for Superconductivity and Department of Physics,*
University of Houston, Houston, Texas 77204, USA
(Dated: April 15, 2013)

Based on the first-principles band structure calculations, we theoretically study the pressure effect on a trivial topological insulator (TI) Sb_2Se_3 and show that there is a topological quantum phase transition occurring from a trivial TI to a non-trivial strong TI at a critical pressure value $P_c \simeq 0.35$ GPa. This pressure induced topological quantum phase transition is confirmed by the bulk energy gap evolution as a function of the pressure, energy band structure with "band inversion", the Z_2 topological invariant, and the existence of the Dirac-like topological surface states. Our calculations can be tested by both spectroscopy and transport experiments.

PACS numbers: 73.43.Nq, 71.15.Mb, 71.70.-d, 73.20.At

The discovery of time reversal invariant (TRI) topological insulators (TIs) [1, 2] has triggered intensive interests in condensed matter community and materials physics. The TIs in two [3, 4] or three [5–15] dimensions have a bulk energy band gap, like an ordinary insulator, but have conducting gapless edge or surface states protected by time reversal symmetry. According to the Kramers theorem, the edge or surface states, consisting of an odd number of massless Dirac cones, are robust against TRI perturbations, while the ones consisting of the even number of massless Dirac cones are not protected. This even-odd effect becomes the key reason why the TI is characterized by a Z_2 topological invariant [5, 16]. On the one hand, when applying the pressure on the Z_2 non-trivial TIs, such as Bi_2Te_3 [17–19] and Bi_2Se_3[20], the superconducting phase will emerge. On the other hand, Sb_2Se_3 is known to be a trivial TI in Bi_2Se_3 family compounds at the ambient pressure. Therefore, there is a question arising as to what will happen when applying the pressure on a trivial TI Sb_2Se_3.

Very recently, the pressure induced transition from a trivial TI to a non-trivial TI in Sb_2Se_3 was observed by the Raman experiment [21]. It is shown that this system undergoes a topological quantum phase transition (TQPT) from a trivial TI phase to a non-trivial one by tuning the pressure. From the theoretical point of view, to reach such a situation of TQPT, four criteria must be satisfied: (i) The bulk energy gap must be closed when the TQPT occurs, namely when the pressure is increased to a critical value P_c, the bulk energy gap should vanish. (ii) The conduction and valence bands cross together forming a "band inversion" at the TRI $\mathbf{k}$ point in the Brillouin Zone (BZ) at a pressure above the critical value P_c. (iii) The Z_2 topological invariant should have a different number in the two phases divided by the bulk energy gap closing point. (iv) The gapless Dirac cone like topological surface state inside the bulk energy gap only exists in one phase, while the other one does not exist. In addition, the mechanism of the pressure induced TQPT observed by Raman experiment [21] remains unclear.

In this Letter, we theoretically study the pressure induced TQPT in Sb_2Se_3 motivated by aforementioned discussions of four fundamental features as well as the mechanism for TQPT based on the first-principles calculations. Firstly, our results show that when the pressure is increased to a critical value $P_c \simeq 0.35$ GPa, which is much smaller than the value of $P_c^e \approx 2$ GPa reported by Raman experiment [21], the bulk energy gap is closed accompanied by the TQPT. Secondly, our study also shows that a "band inversion" appears at the TRI Γ point in BZ at a pressure value above P_c, which is attributed to the pressure induced enhancement of the crystal field splitting, resulting in the anti-crossing between conduction and valence bands. This is the basic physical picture of TQPT induced by the pressure. In order to quantitatively confirm the TQPT indeed occurring at the critical pressure value $P_c \simeq 0.35$ GPa, we calculate the Z_2 topological invariant in two phases separated by the bulk energy gap closing point and show that the low pressure phase has a trivial Z_2 topological invariant number $(0;000)$, while the latter one has the non-trivial Z_2 topological invariant number $(1;000)$. Finally, according to the idea of the bulk-edge correspondence of the TIs, the surface spectral function calculations show that the Dirac like topological surface states inside the bulk energy gap only exists in the high pressure phase, a non-trivial strong TI. The test of these calculations should be readily accessible to both spectroscopy and transport measurements.

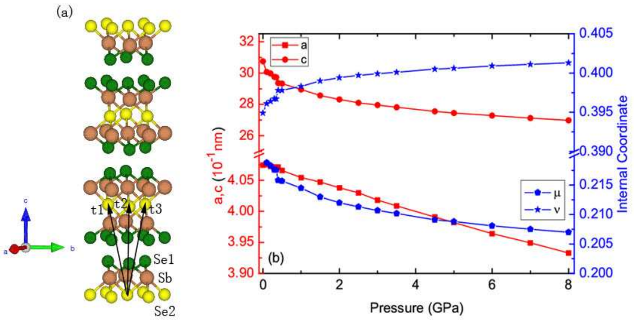

FIG. 1: (Color online) (a) Crystal structure of the Sb_2Se_3 and the primitive translation vectors $\mathbf{t}_{1,2,3}$ are shown. (b) The pressure dependent optimized lattice constants and the internal coordinates of the Sb_2Se_3, where the Se2 site is set to be at the origin $(0, 0, 0)$, the two Sb sites are at $(\pm\mu, \pm\mu, \pm\mu)$, and two Se1 sites are at $(\pm\nu, \pm\nu, \pm\nu)$, defined in the unit of primitive translation vectors, as shown in (a).

The Sb_2Se_3 has a rhombohedral crystal structure with space group $D^5_{3d}(R\bar{3}m)$, as shown in Fig. 1(a). In Fig. 1(a), one can see that the system contains quintuple layers ordered in Se1-Sb-Se2-Sb-Se1 sequence along the c-axis, and the primitive translation vectors $\mathbf{t}_{1,2,3}$ read as $\mathbf{t}_1 = (-a/2, -\sqrt{3}a/6, c/3)$, $\mathbf{t}_2 = (a/2, -\sqrt{3}a/6, c/3)$, and $\mathbf{t}_3 = (0, \sqrt{3}a/3, c/3)$, respectively, where a and c are lattice constants in the hexagonal cell. The internal coordinates of atoms Se1, Se2, and Sb are set to be at the $(\pm\nu, \pm\nu, \pm\nu)$, $(0, 0, 0)$, and $(\pm\mu, \pm\mu, \pm\mu)$, respectively. Without loss of generality, the lattice constants and internal coordinates under the pressure ranged from 0 GPa to 8 GPa without considering the crystal structure phase transition [17, 18, 21] occurring are all optimized based on the first-principles calculations [22] implemented in the VASP code [24]. The optimized results including lattice constants and internal coordinates are all shown in Fig. 1(b). At the ambient pressure P= 0 GPa the optimized lattice constants for Sb_2Se_3 are consistent with those reported by Zhang *et al.* [9]. From Fig. 1(b), we notice that the lattice constants a and c are shrunk with the increasing pressure, as one expects intuitively. However, it is interesting to note that the internal coordinate of Sb atom increases with the higher pressure, which is opposite to what we expect intuitively. However, it can be understood from the binding energy consideration: the coupling is very strong between two atomic layers within one quintuple layer (QL), while the coupling is much weaker between two QLs predominated by the van der Waals type interaction. Consequently, the Sb atoms keep the balance position to minimize the total energy.

We now turn to discuss the relationship between the bulk energy gap and the pressure. As shown in Fig. 2, the calculated bulk energy gap for Sb_2Se_3 at the ambient pressure is 0.24 eV, which is also in good agreement with previous experimental and computational results (about $0.2 - 0.3$ eV) [9, 25, 26]. With the increasing pressure, the bulk energy gap is gradually reduced. Eventually, the bulk energy gap is closed when the pressure is increases to a critical value $P_c = 0.35$ GPa. Due to the fact that the spin-orbit coupling strength in Sb_2Se_3 is not strong enough to induce the band inversion at the ambient pressure, Sb_2Se_3 is maintained as a trivial TI phase at low pressure up to P_c. If the pressure is further increased, the bulk energy gap will be reopened and the system enters an insulating phase again. The bulk energy gap can reach up to a maximal value $E_g \simeq 0.4$ eV with the increasing pressure, which is much larger than the energy scale of room temperature. Such a gap closing-reopening transition by tuning the pressure indicates that there is a phase transition occurring at the critical point P_c.

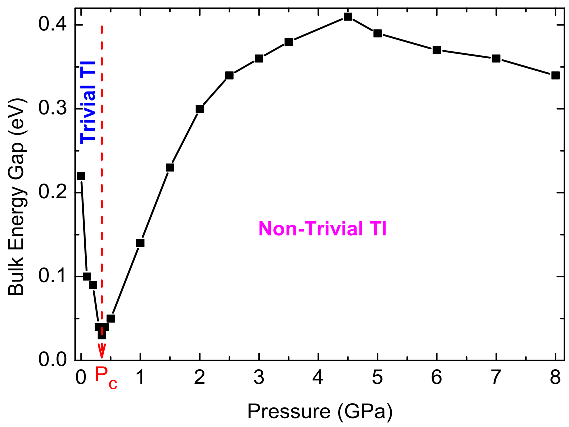

FIG. 2: (Color online) The Phase diagram of the bulk energy gap as a function of the pressure. The red-dashed line denotes the critical point $P_c \simeq 0.35$ GPa of the pressure, at which the bulk energy gap is closed. The low pressure phase is a trivial TI, while the high pressure phase is a nontrivial TI.

In order to understand the nature of the new phase as aforementioned, we also calculate the bulk energy band structure. The energy band structure with and without spin-orbit coupling for the typical pressure values, such as at the ambient pressure and the pressure value with P= 2 GPa, are all shown in Fig. 3. From Fig. 3 we notice that the inclusion of spin-orbit coupling does not lead to a band inversion at the ambient pressure. By comparing with Fig. 3(b) and Fig. 3(d), one can see clearly that the qualitative change is an anti-crossing feature around the Γ point, which indicates an inversion between the conduction band and valence band, suggesting that the new phase in Sb_2Se_3 under high pressure is a non-trivial TI phase. Therefore, we can conclude that the pressure induced phase transition is indeed a TQPT from a trivial TI phase to a non-trivial TI phase.

We now proceed to elaborate the mechanism of the

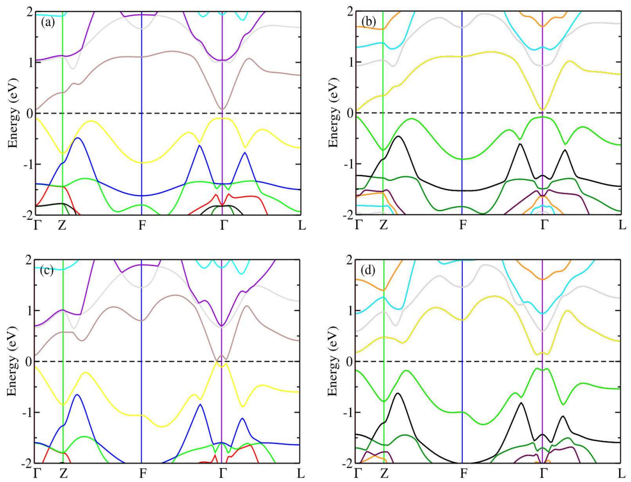

FIG. 3: (Color online) Energy Band structure for Sb_2Se_3 under the pressure P= 0 GPa (a)-(b) and P= 2 GPa (c)-(d). The spin-orbit coupling is taken into account in (b) and (d), while the spin-orbit coupling in (a) and (c) are not included. The dashed line indicates the Fermi level.

pressure induced TQPT. It is known from the atomic physics that the spin-orbit coupling strength is proportional to the atomic number Z^4 ($Z = 51$ for Sb and 34 for Se). As we have shown above, the spin-orbit coupling strength in Sb_2Se_3 is not strong enough to induce the band inversion at the ambient pressure. Therefore, the spin-orbit coupling is unable to induce the band inversion even under the high pressure value and it cannot explain what the experiment observed [21] either. To explore what is the mechanism of TQPT, let us start from the crystal filed splitting without considering the spin-orbit coupling effect. According to the point-group symmetry, the p_z orbital is split from the p_x and p_y orbitals and the latter two orbitals remain degenerate on the Sb and Se atoms. Due to such splitting, the energy levels around the Fermi energy forming the valence and the conduction bands exhibit a large energy gap. This gap is much larger than the energy scale of the spin-orbit coupling at the ambient pressure (compare Fig. 3(a) with Fig. 3(b)). When the pressure is applied, the crystal structure will be squeezed. As a result, the level splitting will be enhanced and the bulk energy gap between the valence band top and the conduction band bottom at Γ point will be gradually reduced. Eventually, the valence band and the conduction band may anti-cross to form a semimetallic state when the pressure is increased to a large value, see Fig. 3(c). In Fig. 3(c), we notice that there are two accidental degenerate states appearing around the Γ point, which is not protected by time reversal symmetry. Consequently, if we further take the spin-orbit interaction into account, these accidental degenerate states will be broken and a non-trivial TI is formed (see Fig. 3(d)).

TABLE I: Parities δ_i at eight TRI $\mathbf{k}$ points for Sb_2Se_3 under different pressure values. The Z_2 topological invariants are $(1;000)$ for a pressure above the critical value P_c while the Z_2 topological invariants are $(0;000)$ for a pressure below the critical value P_c, which indicate a non-trivial strong TI and a trivial TI, respectively.

	δ_1	δ_2	δ_3	δ_4	δ_5	δ_6	δ_7	δ_8	$(\nu_0;\nu_1\nu_2\nu_3)$
0GPa	+1	+1	+1	+1	+1	+1	+1	+1	(0;000)
0.2GPa	+1	+1	+1	+1	+1	+1	+1	+1	(0;000)
0.3GPa	+1	+1	+1	+1	+1	+1	+1	+1	(0;000)
0.4GPa	-1	+1	+1	+1	+1	+1	+1	+1	(1;000)
2GPa	-1	+1	+1	+1	+1	+1	+1	+1	(1;000)
5GPa	-1	+1	+1	+1	+1	+1	+1	+1	(1;000)

To firmly confirm the TQPT nature induced by pressure, we further calculate the Z_2 topological invariant. Because the existence of the spatial inversion symmetry in Sb_2Se_3, the calculation of the Z_2 topological invariant can be dramatically simplified by the so-called "parity method" [27]. Accordingly, the Z_2 topological invariant of Sb_2Se_3 under the pressure environment can be obtained from the wave function parities at the eight TRI $\mathbf{k}$ points defined as $\Gamma_{i=(n_1 n_2 n_3)} = \frac{1}{2}(n_1\mathbf{G}_1 + n_2\mathbf{G}_2 + n_3\mathbf{G}_3)$, where $\mathbf{G}_j$ are primitive reciprocal lattice vectors with $n_j = 0$ or 1, and determined by the quantities

$$\delta_i = \prod_{m=1}^{N_{occ}} \xi_{2m}(\Gamma_i). \tag{1}$$

Here, $\xi_{2m}(\Gamma_i) = \langle \Phi_{2m,\Gamma_i} | \hat{P} | \Phi_{2m,\Gamma_i} \rangle = \pm 1$ is the eigenvalue of parity operator $\hat{P}$ corresponding to even (odd) parity of the Bloch functions at the $2m$-th occupied band and the TRI $\mathbf{k}$ point Γ_i ($i = 1, .., 8$). The sum is taken over all of the occupied bands N_{occ} with only even band index due to the Kramers degeneracy $\xi_{2m} = \xi_{2m-1}$ at the TRI $\mathbf{k}$ point. In Sb_2Se_3 system, there are four independent invariants $(\nu_0;\nu_1\nu_2\nu_3)$,

$$(-1)^{\nu_0} = \prod_{i=1}^{8} \delta_i, (-1)^{\nu_k} = \prod_{n_k=1, n_{j\neq k}=0,1} \delta_{i=(n_1 n_2 n_3)} \tag{2}$$

where ν_0 is the strong topological invariant and independent of the choice of primitive reciprocal lattice vectors $\mathbf{G}_j$ while ν_1, ν_2, and ν_3 defined as weak topological invariants are not. The combination of these four independent invariants $(\nu_0;\nu_1\nu_2\nu_3)$ clearly distinguish three classes of states: non-trivial TI with strong TI and weak TI and trivial TI. The calculated parities δ_i ($i = 1, ..., 8$) at the eight TRI $\mathbf{k}$ points with relative coordinates $(0, 0, 0)$, $(0, 0, 0.5)$, $(0, 0.5, 0)$, $(0, 0.5, 0.5)$, $(0.5, 0, 0)$, $(0.5, 0, 0.5)$, $(0.5, 0.5, 0)$, $(0.5, 0.5, 0.5)$, respectively, in a primitive reciprocal-lattice are listed in Table I. The Z_2 topological invariant $(\nu_0;\nu_1\nu_2\nu_3)$ can be obtained by multiplying over the parities δ_i of all TRI $\mathbf{k}$ points according to Eq.

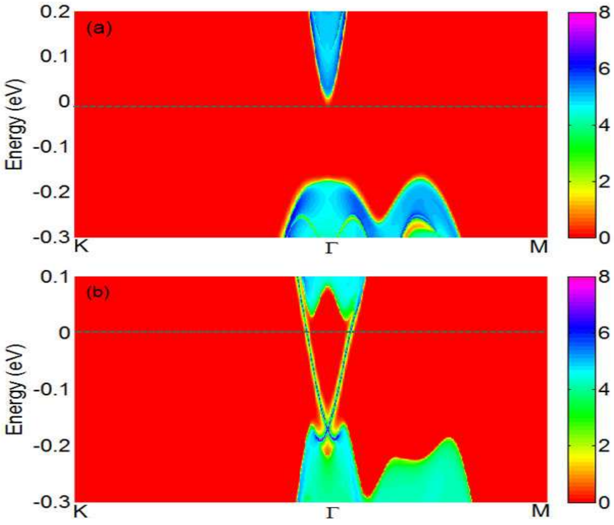

FIG. 4: (Color online) Energy and momentum dependence of the surface spectral function for Sb_2Se_3 with ambient pressure (a) and pressure value P= 2 GPa (b) on the [111] surface. The red regions indicate bulk energy gaps while the green regions indicate bulk energy bands. The Dirac-like topological surface states can only be seen clearly around the Γ point under the pressure P= 2 GPa (lower panel). The dashed line indicates the Fermi level.

(2) and are also listed in Table I. One can see that the Z_2 topological invariants are $(1;000)$ for Sb_2Se_3 at a pressure above the critical value P_c indicating a non-trivial strong TI while Z_2 topological invariants are $(0;000)$ for Sb_2Se_3 at a pressure below the critical value P_c indicating a trivial TI. This agrees with the discussions above that a "band inversion" between the conduction band and valence band occurs at the Γ point. It is also shown that there is a TQPT occurring at the critical pressure value $P_c = 0.35$ GPa.

Finally we discuss the topological surface states based on the idea of the bulk-edge correspondence of the TIs [28]. In order to reveal the topological features of the Sb_2Se_3 system under the pressure, we study the topological surface states of a semi-infinite system with and without the pressure based on the surface Green function [29, 30] constructed by the maximally localized Wannier function fitting to the first principles band structure calculations using the method developed by Marzari and co-workers [31, 32]. The dispersion of the surface states, as shown in Fig. 4, are obtained by evaluating the imaginary part of the surface Green function. By comparison of Fig. 4(a) with Fig. 4(b), one can clearly see the topological surface states, which form a single Dirac cone at Γ point, only exist at the pressure P= 2.0 GPa. This indicates a non-trivial TI nature and agrees well with the bulk parity analysis and band structures calculations.

In conclusion, we have performed the first-principles calculations for the pressure effects on Sb_2Se_3 and shown that there is a TQPT occurring at a critical value $P_c \simeq 0.35$ GPa. To firmly confirm such TQPT, we firstly calculate the bulk energy gap evolution as a function of the pressure and show the bulk energy gap close-reopening transition. Secondly, the band structure calculations show that there is a "band inversion" appearing at the Γ point in BZ at a pressure above P_c, which is attributed to the pressure induced enhancement of crystal field splitting, resulting in the anti-crossing of the conduction and valence bands. Thirdly, the calculated Z_2 topological invariant indicates that a trivial TI phase $(0;000)$ and non-trivial strong TI phase $(1;000)$ is separated by the critical pressure P_c. Finally, the calculated Dirac-like topological surface states only exist in the non-trivial strong TI phase $(1;000)$ region. These results can be tested directly by spectroscopy techniques, such as ARPES and STM, and transport measurements.

We thank R. B. Tao, Z. Fang, X. M. Xie, J.-H. She, B. Gao, D. W. Shen, G. Xu, and Q. S. Wu for helpful discussions. This work was supported by the State Key Programs of China (Grant Nos. 2012CB921604 and 2009CB929204) and the National Natural Science Foundation of China (Grant Nos. 11074043 and 11274069) (W.L.& Y.C.), the National Natural Science Foundation of China No. 61171011 (X.-Y. W.), the Robert A.Welch Foundation under Grant No. E-1146 (C.S.T.), and the National Nuclear Security Administration of the US Department of Energy at LANL under Contract No. DE-AC52-06NA25396 and the US DOE Office of Basic Energy Sciences (J.-X.Z.). W.L. also gratefully acknowledges the financial support by Research Fund of Fudan University for the Excellent Ph.D. Candidates.

[1] M. Z. Hasan and C. L. Kane, Rev. Mod. Phys. **82**, 3045 (2010).
[2] X.-L. Qi and S.-C. Zhang, Rev. Mod. Phys. **83**, 1057 (2011).
[3] B. A. Bernevig, T. L. Hughes, S.-C. Zhang, Science **314**, 1757 (2006).
[4] M. König, S. Wiedmann, C. Brüne, A. Roth, H. Buhmann, L. W. Molenkamp, X.-L. Qi, S.-C. Zhang, Science **318**, 766 (2007).
[5] L. Fu, C. L. Kane, and E. J. Mele, Phys. Rev. Lett. **98**, 106803 (2007).
[6] J. E. Moore and L. Balents, Phys. Rev. B, **75**, 121306 (2007).
[7] R. Roy, Phys. Rev. B **79**, 195322 (2009).
[8] D. Hsieh, D. Qian, L. Wray, Y. Xia, Y. S. Hor, R. J. Cava, and M. Z. Hasan, Nature, **452**, 970 (2008).
[9] H. Zhang, C.-X. Liu, X.-L. Qi, X. Dai, Z. Fang, and S.-C. Zhang, Nature Physics **5**, 438 (2009).
[10] Y. Xia, D. Qian, D. Hsieh, L. Wray, A. Pal, H. Lin, A. Bansil, D. Grauer, Y. S. Hor, R. J. Cava, and M. Z. Hasan, Nature Physics **5**, 398 (2009).
[11] D. Hsieh, Y. Xia, D. Qian, L. Wray, J. H. Dil, F. Meier, J. Osterwalder, L. Patthey, J. G. Checkelsky, N. P. Ong,

A. V. Fedorov, H. Lin, A. Bansil, D. Grauer, Y. S. Hor, R. J. Cava, and M. Z. Hasan, Nature **460**, 1101 (2009).

[12] Y. L. Chen, J. G. Analytis, J.-H. Chu, Z. K. Liu, S.-K. Mo, X. L. Qi, H. J. Zhang, D. H. Lu, X. Dai, Z. Fang, S. C. Zhang, I. R. Fisher, Z. Hussain, and Z.-X. Shen, Science **325**, 178 (2009).

[13] D. Hsieh, Y. Xia, D. Qian, L. Wray, F. Meier, J. H. Dil, J. Osterwalder, L. Patthey, A.V. Fedorov, H. Lin, A. Bansil, D. Grauer, Y. S. Hor, R. J. Cava, and M. Z. Hasan, Phys. Rev. Lett. **103**, 146401 (2009).

[14] W. Zhang, R. Yu, H.-J. Zhang, X. Dai, and Z, Fang, New J. Phys. **12**, 065013 (2010).

[15] C. Chen, S. He, H. Weng, W. Zhang, L. Zhao, H. Liu, X. Jia, D. Mou, S. Liu, J. He, Y. Peng, Y. Feng, Z. Xie, G. Liu, X. Dong, J. Zhang, X. Wang, Q. Peng, Z. Wang, S. Zhang, F. Yang, C. Chen, Z. Xu, X. Dai, Z. Fang, and X. J. Zhou, Proc. Natl. Acad. Sci. USA **109**, 3694 (2012).

[16] C. L. Kane, E. J. Mele, Phys. Rev. Lett. **95**, 146802 (2005).

[17] J. L. Zhang, S. J. Zhang, H. M. Weng, W. Zhang, L. X. Yang, Q. Q. Liu, S. M. Feng, X. C. Wang, R. C. Yu, L. Z. Cao, L. Wang, W. G. Yang, H. Z. Liu, W. Y. Zhao, S. C. Zhang, X. Dai, Z. Fang, and C. Q. Jin, Proc. Natl. Acad. Sci. USA **108**, 24 (2011).

[18] C. Zhang, L. Sun, Z. Chen, X. Zhou, Q. Wu, W. Yi, J. Guo, X. Dong, and Z. Zhao, Phys. Rev. B **83**, 140504(R) (2011).

[19] J. Shen, Y. Ding, Y. Pang, F. Yang, F. Qu, Z. Ji, X. Jing, J. Fan, G. Liu, C. Yang, G. Chen, and L. Lu, arXiv:1303.5598 (2013).

[20] P. P. Kong, J. L. Zhang, S. J. Zhang, J. Zhu, Q. Q. Liu, R. C. Yu, Z. Fang, C. Q. Jin, W. G. Yang, X. H. Yu, J. L. Zhu, Y. S. Zhao, arXiv:1303.0224 (2013).

[21] A. Bera, K. Pa, D.V. S. Muthu, S. Sen, P. Guptasarma, U. V. Waghmare, and A. K. Sood, Phys. Rev. Lett. **110**, 107401 (2013).

[22] In the first-principles calculations, the plane wave basis method, and the Perdew-Burke-Ernzerhof exchange correlation potential[23] has been used. Additionally, the spin-orbit coupling is also included through all over the calculations. A 500eV cutoff in the plane wave expansion and a $12 \times 12 \times 12$ Monkhorst-Pack k-grid are chosen to ensure the calculation with an accuracy of 10^{-5}eV, and all structures (lattice constants as well as internal coordinates) were optimized until forces on individual atoms were smaller than 0.005eV/Å to obtain sufficient accuracy throughout the calculations.

[23] J. P. Perdew, K. Burke, and M. Erznerhof, Phys. Rev. Lett. **77**, 3865 (1996).

[24] G. Kresse and J. Furthmuller, Phys. Rev. B **54**, 11169 (1996).

[25] J. Black, E. M. Conwell, L. Seigle, and C. W. Spencer, J. Phys. Chem. Solids **2**, 240 (1957).

[26] E. Mooser, W. B. Pearson, Phys. Rev. **101**, 492 (1956).

[27] L. Fu and C. L. Kane, Phys. Rev. B **76**, 045302 (2007).

[28] Y. Hatsugai, Phys. Rev. Lett. **71**, 3697 (1993).

[29] M. P. L. Sancho, J. M. L. Sancho, J. M. L. Sancho, and J. Rubio, J. Phys. F **15**, 851 (1985).

[30] W. Li, J. Zang, and Y. Jiang, Phys. Rev. B **84**, 033409 (2011).

[31] N. Marzari and D. Vanderbilt, Phys. Rev. B **56**, 12847, (1997).

[32] I. Souza, N. Marzari, and D. Vanderbilt, Phys. Rev. B **65**, 035109 (2001).